Spectral Color Image Segmentation Using Hidden Markov Models

V. Bochko, J. Parkkinen,* M. Hauta-Kasari,* T. Jaaskelainen**; * Department of Computer Science and Statistics, University of Joensuu; P.O. Box 111, FIN-80101 Joensuu, Finland; **Department of Physics, University of Joensuu; P.O. Box 111, FIN-80101 Joensuu, Finland*

Abstract

In this paper, we propose an approach based on a hidden Markov model (HMM) which accounts for the structure of a spectrum for unsupervised image segmentation. We compute feature sequences representing spectra for training and testing the HMM. In our study, each HMM models one class of a spectral color image. The algorithm computes the model parameters and the discrimination information between the HMMs. The experiments show that the proposed approach gives promising results.

Introduction

Partitioning the image into constituent components is an important research field awakening increasing interest. Regardless of the many automatic learning-based techniques proposed in the literature, segmentation remains a difficult task particularly for spectral color images where each pixel is presented in a multidimensional space. On the other hand, the use of spectral images is very attractive in comparison with conventional color approaches. In the case of spectral images the image regions can be accurately segmented because more spectral bands are available.

While there are many studies devoted to image segmentation based on k-means clustering, Mean Shift, Expectation-Maximization and spectral graph theory [2], [4], [5], [17], learning in sophisticated models requires the use of graphical models like Bayesian networks and Markov random fields (MRF) [6], [7]. In the context of MRF, the image is considered as a noisy observation where the segmentation has to be implemented. Although an extension of this approach to spectral data exists [12], the Markov random fields generally involve analyzing the spatial organization of the data. Another advanced technique, the hidden Markov model (HMM), represents the structure of statistics offering the possibility to learn from complex data [3], [8], [11], [13], [18]. However, the studies presented in [11], [13] and [18] consider only color information and do not incorporate the structural information presented in spectral colors. A 3-D hidden Markov model proposed in [9] was tested only for image segmentation of synthetic volume image models.

In this paper, we construct an HMM-based system incorporating the structure of a spectrum for unsupervised image segmentation. We assume that this spectrum consists of straight-line segments. Thus, it is determined by the sequence of structural line segments or the feature vector sequence. We relate the HMM state to each line segment. We adopt the approach proposed in [3], where each class is modeled by one HMM which is first created and then trained. The approach presented in [3] works with spatial information (textures features) extracted by using Law's masks. The probability density of the feature vector is a multivariate Gaussian distribution. The segmental k-means algorithm is used for training. In this study, spectral information is utilized. Since we have discrete observation symbols we assume a multinomial (discrete) distribution for observations. The Baum-Welch algorithm is used for training. The algorithm defines the number of HMMs and computes the model parameters and the discrimination information between the HMMs. The conducted experiments confirm the feasibility of the method.

Methodology

Preprocessing and Feature Extraction

The preprocessing stage includes scaling on the spectra, which reduces variations in the spectra. We use scaling to obtain the spectral values in the range [0, 1]. However, for spectra corresponding to a white (gray and black as well) color scaling is not usually feasible. Therefore, we first recognize a white (gray, black) color by converting the spectrum into the RGB color space and comparing a color vector with a reference white vector. If a dot product between those two unit norm vectors is greater than the threshold, then the given spectrum represents a white color. Otherwise, we implement scaling on the data.

To utilize a sequential analysis in spectral data we have to introduce the past and the future into the spectral domain. The past relates to the short wavelength subrange. The future corresponds to the long wavelength subrange. To define the spectrum structure we propose to divide the spectral range into several equal intervals where line segments approximate spectrum. The smooth character of spectra of natural objects suggests this choice [14], [10]. The reflectance spectra of natural objects have a dimensionality estimated at between four and seven [1]. This requires the 15 or more channels for spectral measurements. Since linear approximation of spectra is more accurate than stepwise one the number of linear segments used in our study is eight or nine. Each interval represents one observation. The line segment then fits spectrum samples in each interval. The first eigenvector (unit norm) of eigendecomposition is utilized for computing the line segment.

For example, we predefine the eight reference vectors representing all possible variations in the spectrum change using the circle diagram shown in Fig. 1. Fig. 1 shows the spectrum of the blue color presented by the 80 samples. To make an appropriate change of spectra for eigendecomposition we scale the wavelength coordinate to provide the sample values within the interval in the range [0, 10/80]. Each line segment (the first eigenvector) found during spectral analysis is mapped into the circle diagram. The line segment considered as an input vector is then associated with one of the reference vectors. To do this we classify the input vectors using the subspace method. The corresponding algorithm computes the dot products between the input vector and each reference vector. The algorithm then selects the largest value among all products and finds the reference vector index. Fig. 1 shows the enumeration order for the reference vectors (HMM states) from 1 to 8. Thus, the spectral code represents an observation (feature) sequence of eight numbers, each with the values from one to eight.

Hidden Markov Model

The HMM is a Markov chain where the state sequence is hidden and can only be observed through the observation sequence. The HMM is typically characterized and defined by the following: state transition probabilities $A = \{a_{ij}\}$, a probability

density $B = \{b_j(o_t)\}$ of observation o_t given state $q_t = j$, initial state probabilities $\Pi = \{\pi_i\}$, the number of states N and the observation sequence $O = \{o_t\}$, $t = 1,2,\ldots,T$. Given the number of states N and the number of observations T, the parameters A, B and Π represent the model λ, $\lambda = (A,B,\Pi)$. We use the HMM with a discrete density of observations.

Training

Our purpose is to adjust the model parameters to maximize the likelihood of the density function as follows:

$$P(O|\lambda) = \sum_q \pi_{q_1} b_{q_1}(o_1) \prod_{t=2}^{T} a_{q_{t-1}q_t} b_{q_t}(o_t), \quad (1)$$

where summing is obtained over all possible state sequences q. The Baum-Welch algorithm estimates the parameters in Eq.1. For a given training set the algorithm guarantees a monotonic increase of the likelihood function.

Classification

We use one HMM for each class of spectral colors. We assume that there are M classes and M hidden Markov models λ_m, $m = 1,2,\ldots,M$. For classification purposes we use the Viterbi algorithm, which classifies the observation sequence

$$m^* = \arg\max_m P(O|\lambda_m), \quad (2)$$

where m^* is a class to which the observation sequence O belongs.

Discrimination Information

The discrimination information (DI) (symmetry measure) between two HMMs λ_i and λ_j [3], [15] is computed as follows:

$$D_s(\lambda_i,\lambda_j) = \frac{D(\lambda_i,\lambda_j) + D(\lambda_j,\lambda_i)}{2}, \quad (3)$$

$$D(\lambda_i,\lambda_j) = \frac{1}{T}\frac{1}{N}\sum_{k=1}^{N} \left| \log P(O_k^j|\lambda_i) - \log P(O_k^j|\lambda_j) \right|, \quad (4)$$

where $O_k^j = \{O_{k_1}^j, O_{k_2}^j, \ldots, O_{k_T}^j\}$ is a k^{th} observation sequence generated either by model λ_i or λ_j , and N is the number of observation sequences.

System Diagram

The flow chart of the proposed segmentation method is shown in Fig. 2. First, we extract the feature sequences of each spectrum in the image. We then compute the probabilities that the input observation (feature sequence) belongs to each class defined by the HMM, and then select the most probable model (class) using a selection scheme. Finally, we use the postprocessing stage to reduce the classification noise by using median filtering for the labeled image.

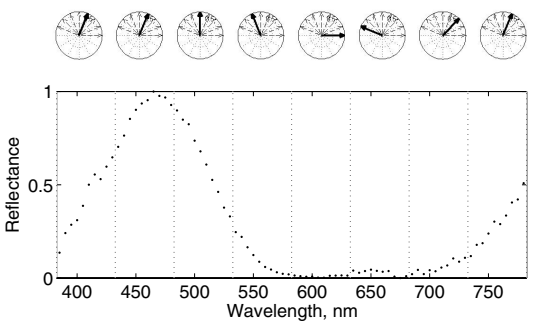

Figure 1. *The scaled spectrum and corresponding eight reference vectors (on the top). The eight reference vectors placed in a circle diagram. The thick line shows the recognized reference vector. The observation sequence is 44561834. In our approach the reference vector orientation is important while the reference vector direction is not.*

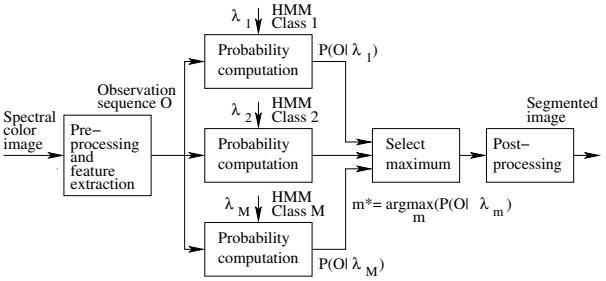

Figure 2. *The system diagram of the proposed method including preprocessing, feature extraction, HMMs, class selection, and postprocessing.*

Feature extraction involves computing the line segments in the spectrum. Thus, each feature vector codes spectral structural information. We then use the approach presented in [3], based on two-stage segmentation (coarse and fine) using the merging technique. While the coarse segmentation is region-based, the fine segmentation is pixel-based. For coarse segmentation we divide the entire image area into a number of non-overlapped equal-sized square regions. One HMM learns from each region. To provide the coarse segmentation, we merge the HMMs representing the same class if the DI between the models is less than a threshold. Consequently, we reduce the number of HMMs to approximate the number of HMMs relevant for image segmentation and adjust the model parameters. The threshold value is experimentally defined. For fine segmentation the observation sequence of each spectral pixel is tested against all HMMs defined from the coarse segmentation stage. This procedure labels all pixels and provides the segmentation of the image.

Experiments

We conducted experiments with eight spectral images pens ($100 \times 141 \times 81$, $380:5:780$), cherry ($113 \times 176 \times 81$, $380:5:780$), sungirl ($95 \times 150 \times 81$, $380:5:780$), cars ($256 \times 160 \times 81$, $380:5:780$), bra ($131 \times 141 \times 81$, $380:5:780$), fruits ($160 \times 120 \times 81$, $380:5:780$), flowerY ($300 \times 250 \times 44$, $420:7:721$) and flowerR ($300 \times 250 \times 44$, $420:7:721$). The numbers in parentheses are the image size: width, height and spectral dimension, and the wavelength range: minimum, interval and maximum. We remove one dimension for the images with a spectral dimension of 81 (eight linear segments) and extrapolate one dimension for images with a spectral dimension of 44 (nine linear segments). The test images were acquired using different spectral cameras, at different time, places and illumination conditions. Fig. 4 shows color reproduction of the test images.

We use the parameters given in Table 1, where the *ID threshold* denotes a threshold for elements of $D_s(\lambda_i,\lambda_j)$, the *W threshold* denotes one at the preprocessing stage, the row *observations* shows the number of observations and the *region size* defines a size of a square region. Fig. 3 illustrates coarse segmentation, fine segmentation and postprocessing. In Fig. 3b the black color regions have ambiguous meanings. In the postprocessing stage we compute the median filtering values for the segmented image with gray-level labels and then relate each gray level to a corresponding color.

Fig. 5 shows segmentation results by the proposed method. Though the results are varied for the proposed approach at each launching of the algorithm, in general the results are similar. The results indicate that the proposed method generates relevant spectral color labels in most cases. The regions in HMM segmentation are coherent. Although the object edges are cor-

rupted, the results for the HMM are rather good. The HMM-based approach automatically selects the number of classes. Scaling the spectra at the preprocessing stage reduces color variations inside color objects while the recognition of white, gray, and black colors removes the shadow variations for the background. In addition, Fig. 5 shows the results and indicates from that the foreground objects are segmented relatively well and presented in the relevant colors. The background has less appropriate color due to the low contrast and less colorfulness. After postprocessing some of the images are still noisy.

Table 1:Adjustable parameters for the test images

Images	pens	cherry	sungirl	cars
Number of states	8	8	8	8
Observations	8	8	8	8
Region size	11	11	11	11
ID threshold	3	1	2	5
W threshold	0.9995	0.995	0.9992	0.9992
Median filter size	5×5	5×5	5×5	5×5
Images	bra	fruits	flowerY	flowerR
Number of states	8	8	8	8
Observations	8	8	9	9
Block size	11	11	11	16
ID threshold	6	1.1	1	0.35
W threshold	0.994	0.9995	0.995	0.9995
Median filter size	5×5	5×5	7×7	5×5

The Rand index is then used for quantitative comparing segmentations by the proposed algorithm and hand-labeled ground-truth segmentations [16], [19]. The Rand index counts the pairs of pixels that have compatible label relationships in two segmented images. The Rand index is 1 if two partitions agree perfectly. Therefore a higher value of the Rand index is desirable. Fig. 6 shows a set of manually segmented images. Table 2 shows the Rand index for the test images. One can see that the results vary for different images. The image bra has the best value and segmentation of the image cherry is not so good.

Finally, we note that the Baum-Welch algorithm used for training is time consuming. This makes it difficult to find correct parameters for segmentation. In addition, the Baum-Welch algorithm may get stuck at local maximum. In our future work we will consider more efficient approaches for noise removal and training.

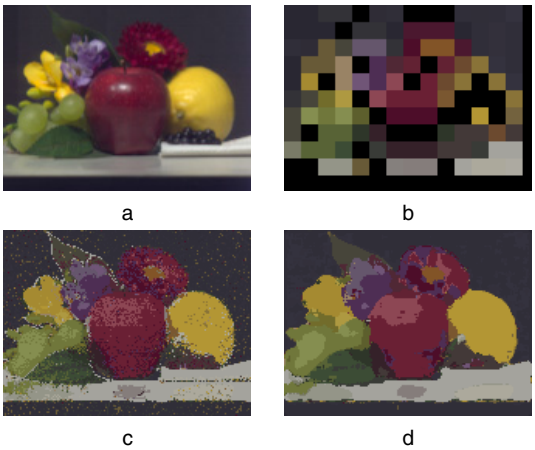

Figure 3. *Segmentation result using the proposed method for the image fruits. a) RGB color reproduction of the original spectral color image. b) Coarse segmentation. c) Fine segmentation. d) Postprocessing.*

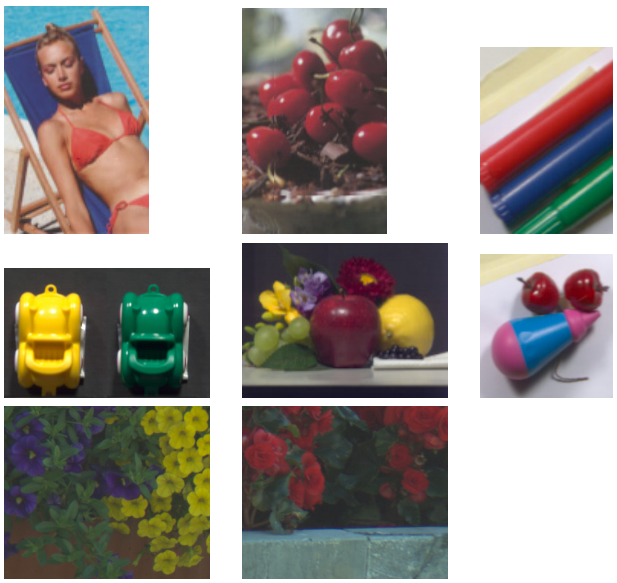

Figure 4. *RGB color reproduction of test images (from left-top to right-bottom): sungirl, cherry, pens, cars, fruits, bra, flowerY and flowerR.*

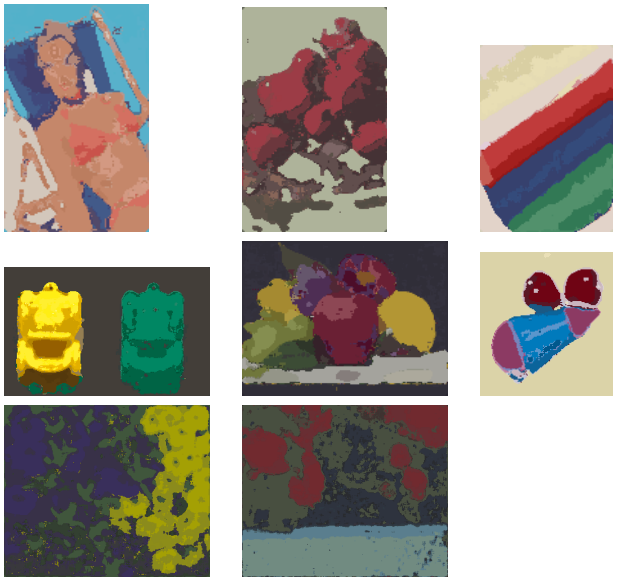

Figure 5. *Segmentation results by the proposed method.*

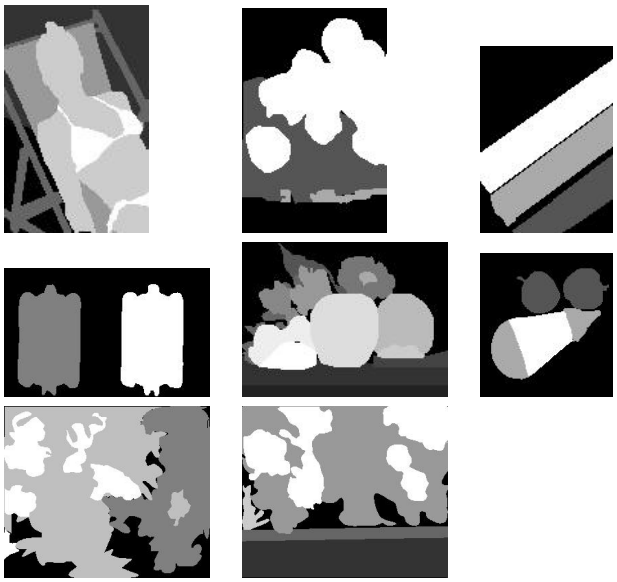

Figure 6. *Manual segmentations of test images.*

Table 2: Rand index

Images	Rand index
pens	0.77
cherry	0.71
sungirl	0.82
cars	0.84
bra	0.92
fruits	0.87
flowerY	0.74
flowerR	0.82

Conclusions

We proposed the unsupervised segmentation approach for spectral color images. The approach involves learning with HMMs and pixel-based recognition in spectral images. Given the threshold for the DI, the approach automatically finds the number of classes. The regions segmented by the proposed approach are coherent and have relevant spectral color labels. The drawback is that the algorithm is time consuming. We demonstrated the effectiveness of the proposed method by conducting experiments on eight spectral color images.

References

[1] H. Altunbasak, and H. J. Trussell, Colorimetric Restoration of Digital Images, IEEE Trans. Image Processing, 10, (3), pp. 393-402 (2001).

[2] C. M. Bishop, Pattern Recognition and Machine Learning, Springer, 2006.

[3] J.-L. Chen and A. Kundu, Unsupervised Texture Segmentation Using Multichannel Decomposition and Hidden Markov Models, IEEE Trans. Image Processing, 4, (5), pp. 603-619 (1995).

[4] D. Comaniciu and P. Meer, Mean Shift: A Robust Approach Toward Feature Space Analysis, IEEE Trans. Pattern Analysis and Machine Intelligence, 24, (5), pp. 603-619 (2002).

[5] A. P. Dempster, N. M. Laird, and D. B. Rubin, Maximum Likelihood from Incomplete Data via the EM Algorithm, Royal Statistics, B, (39), pp. 1-38 (1977).

[6] R. C. Dubes and A. K. Jain, Random Field Models in Image Analysis, J. Applied Statistics, 16, (2), pp. 131-164 (1989).

[7] S. Geman and G. Geman, Stochastic Relaxation, Gibbs Distributions and the Bayesian Restoration of Images, IEEE Trans. Pattern Analysis and Machine Intelligence, 6, pp. 721-741 (1984).

[8] Y. He and A. Kundu, 2-D Shape Classification Using Hidden Markov Model, IEEE Trans. Pattern Analysis and Machine Intelligence, 13, 11, pp. 1172-1184 (1991).

[9] D. Joshi, J. Li and J. Z. Wang, A Computationally Efficient Approach to the Estimation of Two- and Three- dimensional Hidden Markov Models, IEEE Trans. on Image Processing, 15, (7), pp. 1871-1886 (2006).

[10] E. L. Krinov, Spectral Reflectance Properties of Natural Formations, TT-439, National Research Council of Canada, Ottawa, 1947.

[11] H.-C. Lin, L.-L. Wang and S.-N. Yang, Color Image Retrieval Based on Hidden Markov Models, IEEE Trans. Image Processing, 6, (2), pp. 332-339 (1997).

[12] G. Mercier, S. Derrode and M. Lennon, Hyperspectral Image Segmentation with Markov Chain Model, Proc. IGARSS, pp. 3766 3768 (2003).

[13] S. Muller, S. Eickeler and G. Rigoll, An Integrated Approach to Shape and Color-Based Image Retrieval of Rotated Objects Using Hidden Markov Models, Eds. H. Bunke and T. Caelli, Hidden Markov Models: Application in Computer Vision, World Scientific, pp. 223-237 (2001).

[14] J. Parkkinen, J. Hallikainen, and T. Jaaskelainen, Characteristic Spectra of Munsell Color, J. Opt. Soc. Am. A 6, pp. 318-322 (1989).

[15] L. R. Rabiner, A Tutorial on Hidden Markov Models and Selected Applications in Speech Recognition, Proc. IEEE, 77, pp. 257-286 (1989).

[16] W. M. Rand, Objective Criteria for the Evaluation of Clustering Methods, J. Am. Statistical Assoc., 66, (336), pp. 846-850 (1971).

[17] J. Shi and J. Malik, Normalized Cuts and Image Segmentation, IEEE Trans. Pattern Analysis and Machine Intelligence, 22, (8), pp. 888-905 (2000).

[18] Z. Tu and S.-C. Zhu, Image Segmentation by Data-Driven Markov Chain Monte Carlo, IEEE Trans. on Pattern Analysis and Machine Intelligence, 24, (5), pp. 657-673 (2002).

[19] R. Unnikrishnan, C. Pantofaru and M. Hebert, A Measure for Objective Evaluation of Image Segmentation Algorithms, Proc. CVPR Workshop Empirical Evaluation Methods in Computer Vision, 3, pp. 34-41 (2005).

Author Biography

Vladimir Bochko received his PhD from St. Petersburg State Electrical Engineering University, Russia (1987). Since 2007 he has worked in the Department of Computer Science and Statistics, University Joensuu, Finland. His research interests are in color and image analysis. He is a member of the Finnish Pattern Recognition Society.